ORIGINAL PAPER

Structural, morphological, nonlinear optical and power limiting properties of acid green 3 dye-doped PVA films

S Hemalatha and T Geethakrishnan*

Department of Physics, University College of Engineering Villupuram (A Constituent College of Anna University), Villupuram 605103, Tamilnadu, India

Abstract: Acid green 3 (AG 3) dye-doped poly(vinyl alcohol) (PVA) films were formed on microglass slides via solution casting technique; their structural, morphological, linear, nonlinear optical and power limiting characteristics were studied. AG 3-PVA films were characterized by UV–visible spectroscopy, Fourier transform infrared (FT-IR) spectroscopy, atomic force microscopy and scanning electron microscopy methods. The nonlinear optical absorption and refraction properties of AG 3-PVA films were studied by Z-scan technique using a 5 mW diode laser of 635 nm wavelength. AG 3-PVA films were found to exhibit a consistent reverse saturable absorption phenomenon and negative optical nonlinearities; their $\chi^{(3)}$ values were measured to be of the order of 10^{-5} esu and optical power limiting behavior was also observed for these films. Based on the results of the present experimental work, we suggest that AG 3-PVA films may be suitable for optical limiting, photonic and optoelectronic applications in the low-power regime.

Keywords: Acid green 3 dye; PVA films; Nonlinear optics; Z-scan; Optical limiting

1. Introduction

Organic molecule-based polymer materials or photosensitive materials show high interest due to their potential applications in optical communications, optical data storage, optical limiting, optical signal processing and computing, etc [1–3]. Organic nonlinear optical (NLO) materials possess unique optical properties, such as fast response time, broad wavelength range, low optical loss and high optical nonlinearities, which are being used to design several photonic and optoelectronic devices [4–7]. Polymer materials play a major role in the field of optics and optoelectronics, which form an excellent platform of host materials for metal ions, organic and inorganic compounds, etc. These materials possesses unique properties such as high flexibility, durability, low density, better thermal stability and works well for over a range of visible spectrum of light [8–13]. Embedding organic chromophores with host polymers have proved to be the efficient and affording materials for organic light-emitting diodes (OLEDs), solar cells, optical limiters and NLO devices [14, 15]. Organic dye molecule-incorporated

polymer materials are well suited for designing NLO devices due to their low cost, higher nonlinear index of refraction, easier fabrication and biodegradable qualities [16]. Plenty of NLO materials are already available in the recent studies, which utilize (vinyl polymer) polyvinyl alcohol (PVA) due to its excellent film-forming ability, compatibility, water solubility and high dielectric strength [17]. Soliman et.al. [18] have recently reported the structure and linear optical properties of pure PVA and PVA filled with Fe nanoparticles. Ali and Kersh [19] have reported the structure and optical properties of Ce^{3+} ion-doped PVA and PVP composite films. I.Qashou et.al reported the methylsilicon phthalocyanine hydroxide-doped PVA films and their optical and electronic properties for applications in photovoltaic devices and solar cell [20].

The present work aims to prepare acid green 3 dye polyvinyl alcohol (AG 3-PVA) films, exploring their structure and morphology and to study their linear and nonlinear optical properties. Acid green 3 dye (molecular formula of $C_{37}H_{35}N_2NaO_6S_2$, color index: 42085) appears as dull dark green powder and belongs to triarylmethane dye family. This dye has been extensively used for dyeing silk or wool, wood fabrics, pigments and paper industries, etc. The molecular structures of the acid green 3 dye molecule are illustrated in Fig. 1a. PVA (molecular weight

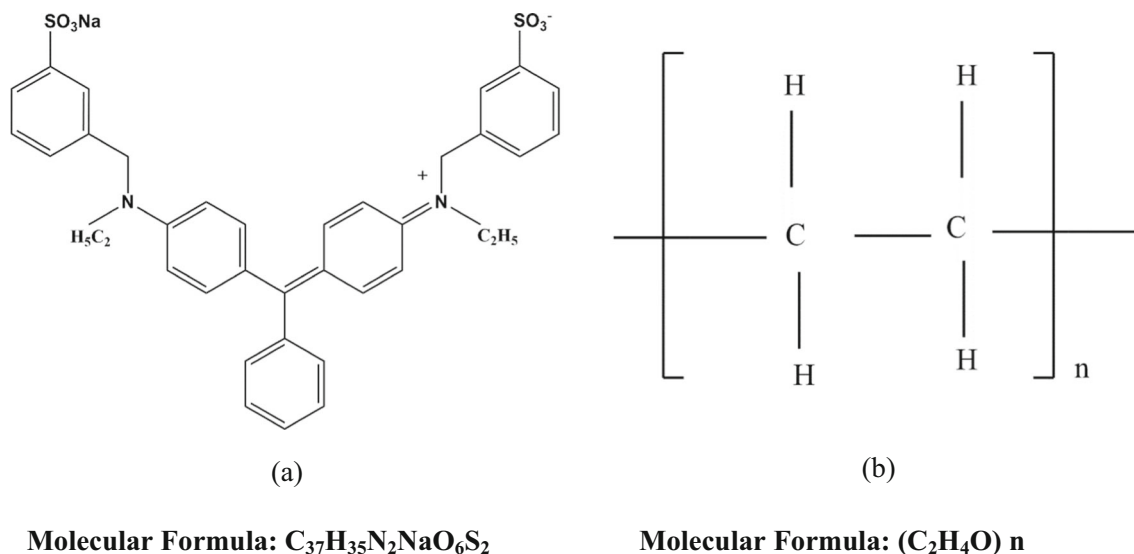*Corresponding author, E-mail: tgeethakrishnan@hotmail.com

(a)   (b)

Molecular Formula: C$_{37}$H$_{35}$N$_2$NaO$_6$S$_2$ **Molecular Formula: (C$_2$H$_4$O) n**

Fig. 1 Structure and molecular formula of (**a**) acid green 3 dye (**b**) PVA

of 125,000 g mol^{-1}) is a non-toxic, chemical-resistant, biocompatible and biodegradable polymer with good adhesive quality [21]; further, PVA is mainly used in medicinal field due to its low-protein-adsorption characteristics. The existence of hydroxide (OH) groups and (H) hydrogen bond formation in PVA determines its physical, chemical and mechanical properties. PVA has been used as a host template for preparing the AG 3-PVA films utilized in the present experimental work; the molecular structure of PVA is shown in Fig. 1b. The host polymers provide an ideal strategy and offer smooth interaction with the embedded guest molecules, which can alter the properties of the organic dye molecules; the nonlinear optical characteristics of this kind of materials can be investigated to fabricate the suitable NLO devices.

2. Experimental details

2.1. Materials and preparation of AG 3-PVA films

The high-analytical-grade compounds of PVA and AG 3 dye were purchased from Sigma-Aldrich. The solution casting technique has been used to prepare the AG 3-PVA film samples, which is the most preferred method because of its easiness and cost-effectiveness. A known weight of PVA (2 wt%) was dissolved in distilled water at 90 °C and stirred for 2 hours with the help of magnetic stirrer until the polymer got dissolved completely to get clear solution. Later, the solution was cooled down to room temperature under continuous stirring. A weighed amount of different concentrations of AG 3 dye (0.01 mM, 0.02 mM and 0.03 mM) were then incorporated into the clear solution

under stirring for 1 h to get the homogenous solution. AG 3 dye-PVA mixtures of different concentrations were then casted on perfectly leveled glass microslides. The glass substrates were kept in dark, dust-free environment for better film formation. The film thickness is in the range from 16 to 28 μm, and the prepared AG 3-PVA films were characterized for further investigations.

2.2. Characterization methods

The linear absorption spectra of AG 3-PVA films are acquired using a Perkin–Elmer Lambda 35 spectrophotometer. The FT-IR spectra of the AG 3-PVA films were obtained using a Perkin–Elmer infrared spectrometer with an attenuated total reflectance (ATR) of cm^{-1} resolution in the wave number range of 4000–400 cm^{-1} in transmittance mode. The surface morphology and microstructural analysis of these films were recorded using the scanning electron microscopy (SEM) (CAREL ZEISS-EVO 18) and atomic force microscopy (AFM) in contact mode method (Digital instruments Nanoscope E, with Si$_3$N$_4$ 100 μm cantilever of force constant 0.58 Nm^{-1}).

The Z-scan technique, developed by Sheik Bahae et al. [22] works based on the principle of spatial beam distortion of the Gaussian beam and this technique is used to study the third-order optical nonlinearity of various kinds of NLO materials. Z-scan experiments were carried out, using a low-power (5 mW) continuous-wave (CW) diode laser of 635 nm wavelength, in order to measure the optical nonlinearities of AG 3-PVA films. The nonlinear coefficient of absorption and the nonlinear index of refraction of AG 3-PVA films were determined, respectively, by performing the open-aperture and closed-aperture Z-scan

measurements utilizing the experimental arrangement as shown in Fig. 2. The light from the laser was made to focus on AG 3-PVA films by a 5 cm convex lens and this leads to a beam waist of (ω_0) and Rayleigh length (Z_R) of 16.75 μm and 1.38 mm, respectively. The intensity of the transmitted beam through the sample was measured simultaneously by a photodetector with (closed) and without (open) aperture in the far field of lens, as the sample was translated across the focal region along z-direction.

3. Results and discussion

3.1. UV–visible study

Ultraviolet–visible spectra of AG 3-PVA films with dye concentrations of 0.01 mM, 0.02 mM, 0.03 mM, unfilled PVA film (inset) and AG 3 dye in water of 0.01 mM (dotted lines) are studied, and the results are shown in Fig. 3. The spectra of unfilled PVA shows an absorption band centered at 300 nm [12]. A negligible absorbance is obtained for the unfilled PVA in the higher-wavelength region of the visible spectrum. In an aqueous solution, AG 3 dye is characterized by the absorption bands centered at 620 nm. AG 3-PVA films exhibit a well-structured and wide absorption band centered at 642 nm. A redshift of 22 nm in the absorption spectra was observed for AG 3-PVA films, over the aqueous solution of AG 3 dye, and may be due to the film formation of AG 3 dye with the PVA molecules [23]. The increase in dye concentration of AG 3-PVA films shows an increase in absorbance which may be due to the possible bonding interaction between the dye and PVA molecules and the corresponding increase in optical densities of the films. The absorption peak observed around 620 nm, for the aqueous solution of AG 3 dye, shifts toward higher wavelengths with different absorption

intensities for AG 3-PVA films (i.e., for different dye concentrations). This may be due to the formation of inter- or intramolecular hydrogen bonding between the AG 3 dye and the OH groups present in the PVA molecules [24].

3.2. FT-IR spectroscopy

The Fourier transform infrared (FT-IR) spectroscopy has been used to characterize the structure and functional groups present in the AG 3-PVA films. Figure 4a to e, respectively, shows the FT-IR spectra of AG 3 dye, unfilled PVA film and AG 3-PVA films with different dye concentrations of 0.01 mM, 0.02 mM and 0.03 mM. The non-appearance of any vibrational absorption bands in the FT-IR spectra of AG 3-PVA films compared to that of unfilled PVA predicts that there is no further formation of covalent bonds between polymer and AG 3 dye [25]. The weak hydrogen bonding interaction between the polymer hosts and the organic dye chromophores is due to the intensity variation of the vibrational bands and shifts observed in the FT-IR spectra. The FT-IR spectrum and their band assignments for unfilled PVA film and AG 3-PVA films are given in Table 1.

3.3. AFM and SEM characterizations

Figures 5a and 6a shows the 2D and 3D surface roughness images in a 25 × 25 μm² of unfilled PVA, and Figs. 5b–d and 6b–d, respectively, shows the AG 3-PVA films of 0.01 mM, 0.02 mM and 0.03 mM concentrations. The crystalline and amorphous portions of polymer surfaces are distinguished in AFM by two categories: (a) light-colored (crystalline) and dark-colored (amorphous matrix) [26]. AFM images recorded for the unfilled PVA show the irregular distribution or molecular rearrangement of polymeric chains exists in amorphous phase. Incorporation of AG 3 dye molecules into PVA shows the proper arrangement of crystallinity and uniform distribution of filler molecules. As the concentration of the dye molecules increases in AG 3-PVA films, the grain size and surface roughness also get increase. The encapsulation process traps the organic dye molecules inside the PVA matrix pores, free volumes, as well as interstitials which minimize the formation of microporosity. The contact mode atomic force microscopy was used to acquire the surface details of AG 3-PVA films, as well as homogeneity and thin film aspects [27]. The observed change in the surface morphology may be attributed to a surface nucleated crystallization of PVA assisted by the filler dye molecules [28].

Figure 7 shows the micrographs recorded for AG 3-PVA films with dye concentrations of 0.01 mM, 0.02 mM and 0.03 mM using scanning electron microscopy, and the images reveal the variation of
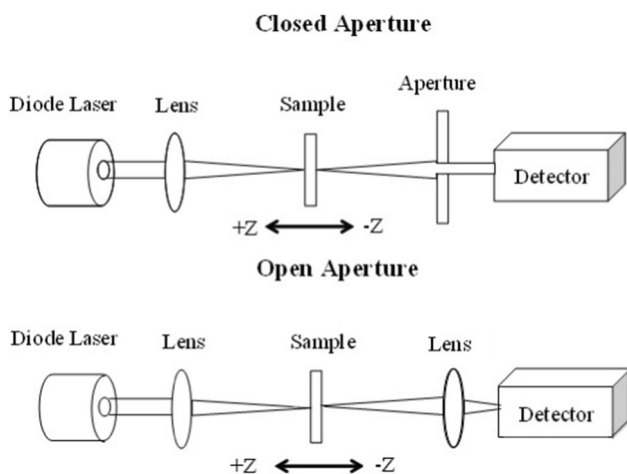

Closed Aperture

Diode Laser   Lens   Sample   Aperture   Detector
+Z ⟷ -Z

Open Aperture

Diode Laser   Lens   Sample   Lens   Detector
+Z ⟷ -Z

Fig. 2 Experimental arrangements of Z-scan

Fig. 3 UV–visible absorption spectra of AG 3-PVA films with dye concentrations of (**a**) 0.01 mM, (**b**) 0.02 mM, (**c**) 0.03 mM, (**d**) AG 3 dye in water of 0.01 mM. *The inset*: PVA film
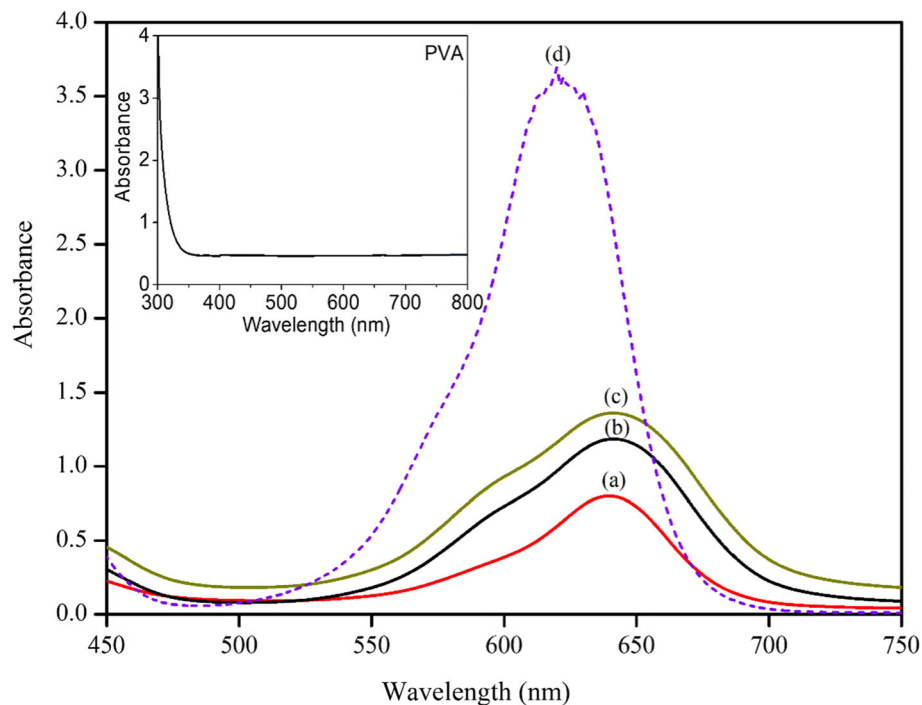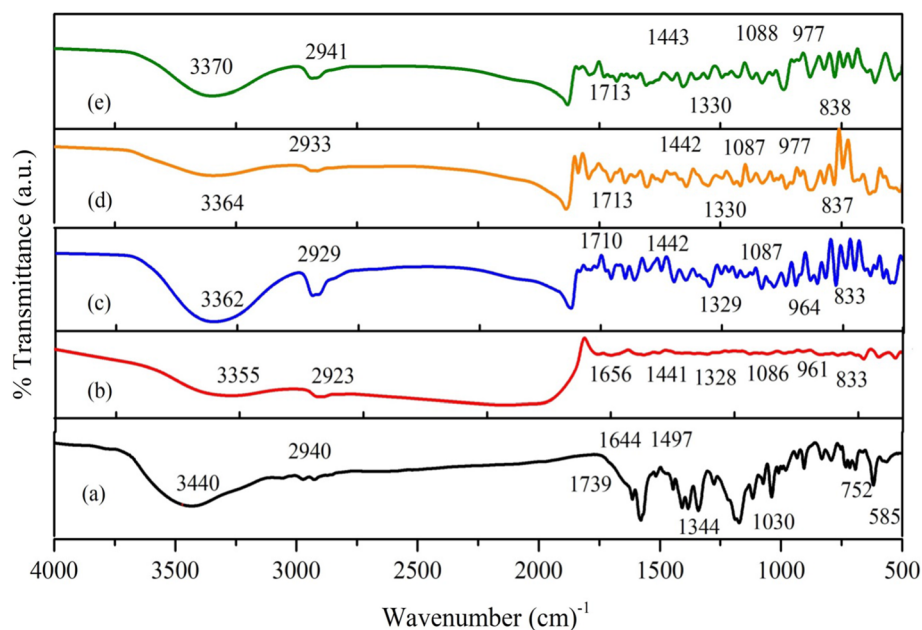
Fig. 4 FT-IR spectra of (**a**) AG 3 dye (**b**) PVA film, (**c**), (**d**) and **e** AG 3-PVA films with dye concentrations of 0.01 mM, 0.02 mM and 0.03 mM

morphological structure. Figure 7a clearly shows that the porosity of the polymer and the dye molecules could not be identified for AG 3-PVA films which contains a well-mixed AG 3 dye and PVA molecules and has a uniform distribution of surface with interconnected network of fibers. Figure 7b shows the clusters of PVA film in which AG 3 dye molecules are bind over polymer matrix to form a network chain of particles. A closely interconnected AG

3 dye molecules coated on the surface of the PVA is observed as the concentration of dye molecules gets increases [29]. With further increase in the dye concentration, an agglomeration of particles is formed on the surface of PVA which exhibits polycrystalline structure with large grain boundaries as shown in Fig. 7c, and from this, it is clear that the grain size depends on the amount of dye molecules bonded with PVA matrix [30, 31].

Table 1 FT-IR peak assignments for PVA and AG 3-PVA films

PVA Peak positions (cm^{-1})	AG 3–PVA (0.01 mM)	AG 3–PVA (0.02 mM)	AG 3–PVA (0.03 mM)	Peak assignments
3355	3362	3364	3370	O–H stretching
2923	2929	2933	2941	Alkyl C-H stretching
1656	1710	1713	1713	C=O stretching
1441	1442	1442	1443	CH$_2$ bending deformation
1328	1329	1330	1330	O–H inplane deformation with C–H wagging
1086	1087	1087	1088	C–O stretching
961	964	977	977	Alkene C=C bending
833	833	837	838	PVA skeletal band

Fig. 5 Two-dimensional AFM images of (**a**) PVA film, AG 3-PVA films with dye concentrations of (**b**) 0.01 mM, (**c**) 0.02 mM and (**d**) 0.03 mM
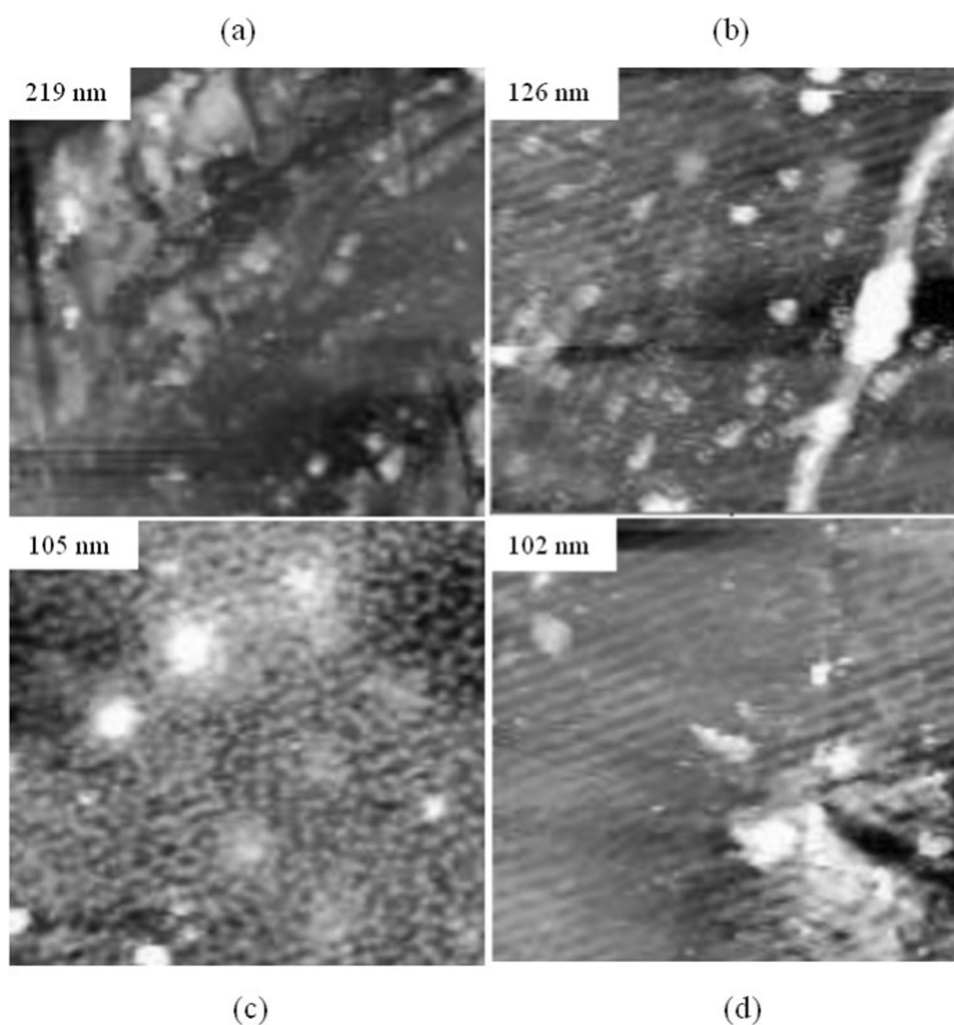
3.4. Z-scan measurements

The two prominent nonlinear absorption (NLA) mechanisms that could occur in organic dyes are saturable absorption (SA) and reverse saturable absorption (RSA). Materials possessing SA characteristics are widely used in mode locking, laser pulse compression, optical bi-stability, optical switches, etc., whereas the materials having RSA properties are applied in optical limiters, 3D optical storage, etc [32–34]. The NLA process was investigated using
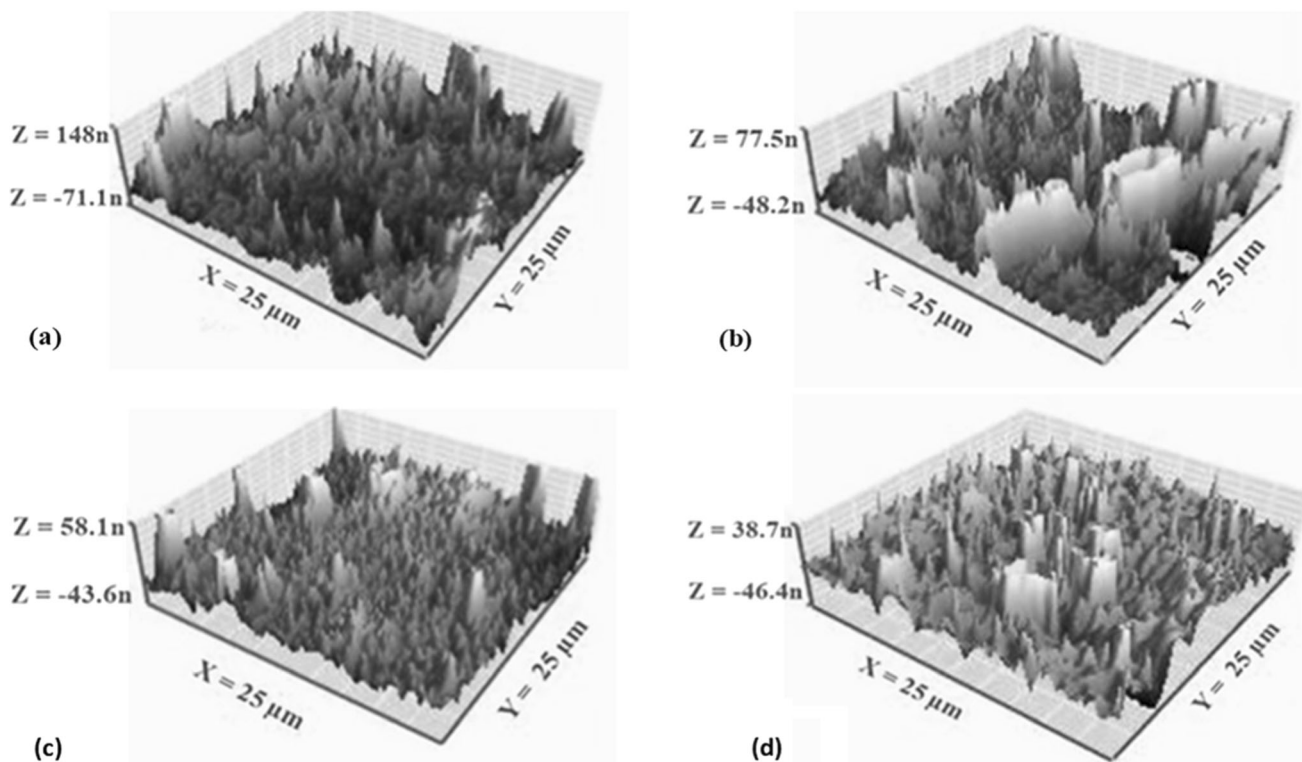
Fig. 6 Three-dimensional AFM images of (**a**) PVA film, AG 3-PVA films with dye concentrations of (**b**) 0.01 mM, (**c**) 0.02 mM and (**d**) 0.03 mM
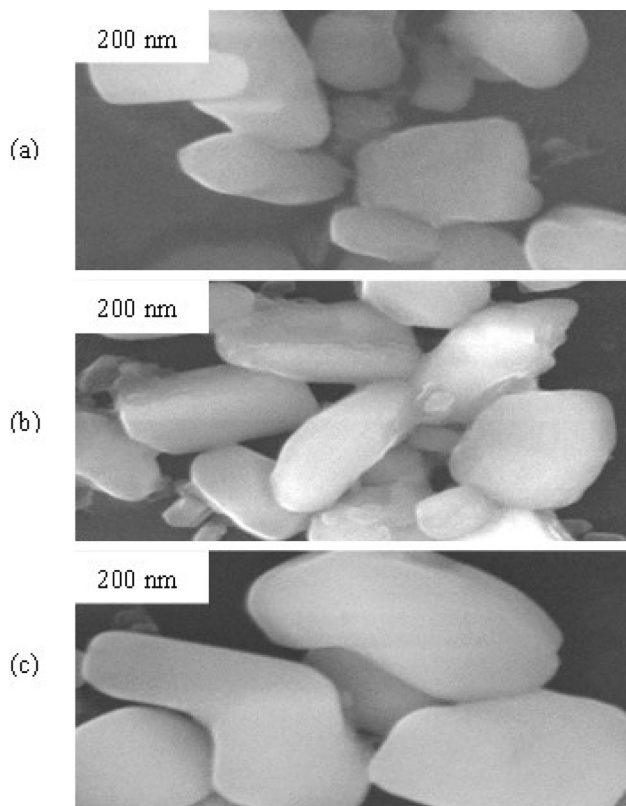

Fig. 7 SEM micrographs of AG 3-PVA films (**a**) 0.01 mM, (**b**) 0.02 mM and (**c**) 0.03 mM

open-aperture (OA) Z-scan measurements for the aqueous solution of AG 3 dye and AG 3-PVA films with different dye concentrations at an incident laser intensity of $I_0 = 1.135 \times 10^3$ Wcm^{-2}, and the corresponding results are presented in Fig. 8. The solid lines represent the theoretical fit obtained using Eq. (2). When the sample is far away from the focus, the incident intensity is low; as the focal intensity increases at the sample, the transmittance of beam increases and this depicts the SA behavior (negative nonlinear absorption). In the case of RSA, when the focal intensity approaches the maximum value at the sample, i.e., near the focus ($z = 0$), the transmittance value gets decreased (i.e., positive nonlinear absorption phenomenon) [35–37]. In the present case, Fig. 8 clearly shows the normalized transmittance curve obtained a deep valley about the focus which indicates the existence of RSA for the entire samples studied and follows the thermal nonlinear process. The outcome of reverse saturable absorption is owing to the some of the nonlinear mechanisms such as two-photon absorption (TPA), excited state absorption (ESA), free carrier absorption (FCA) and reverse saturable absorption (RSA), nonlinear scattering or with the pattern of these process. Generally, RSA is based on: (i) the incident photon of the same wavelength can be absorbed by molecules in both ground and excited states and (ii) the excited state absorption must be greater than ground state
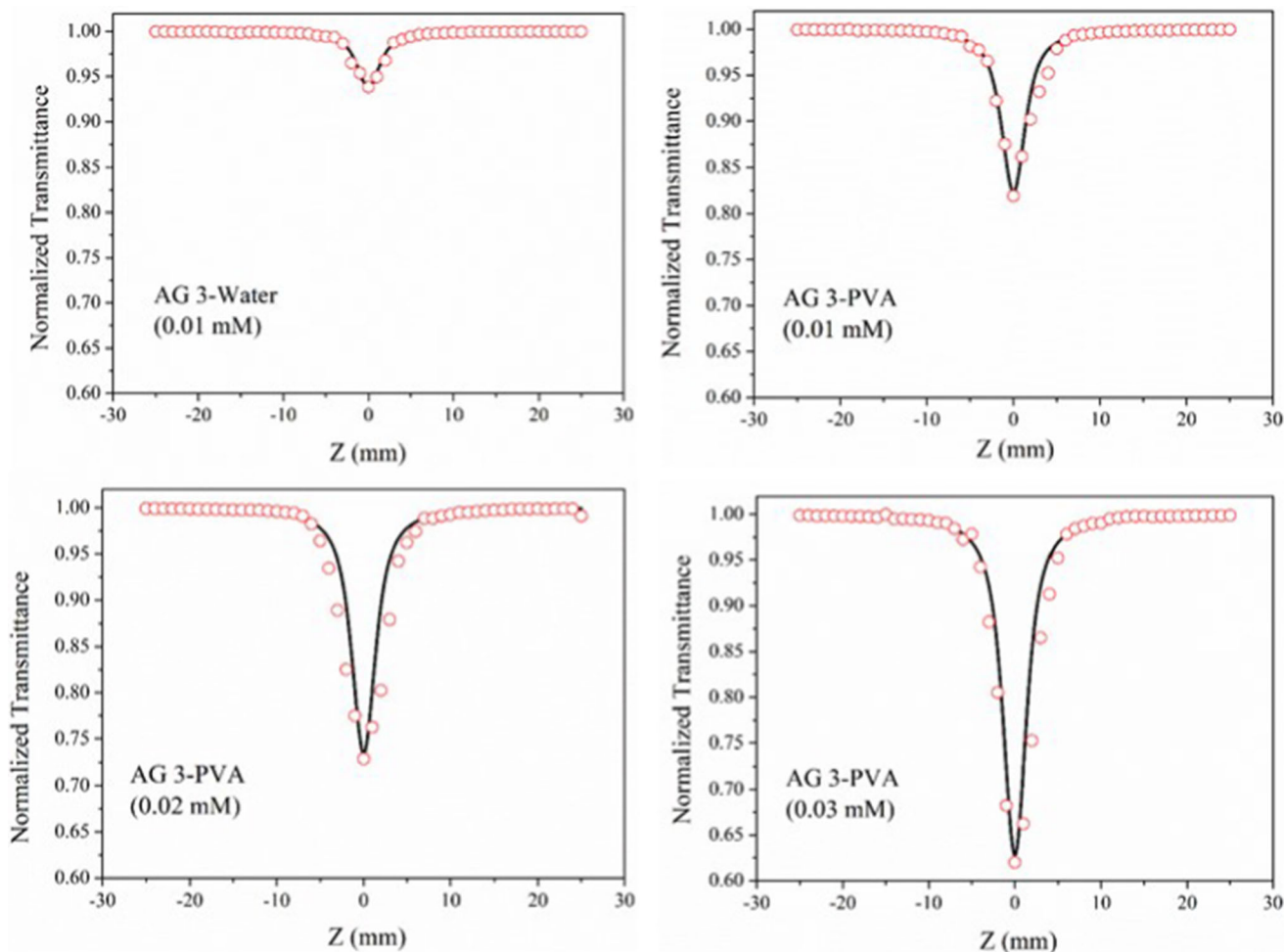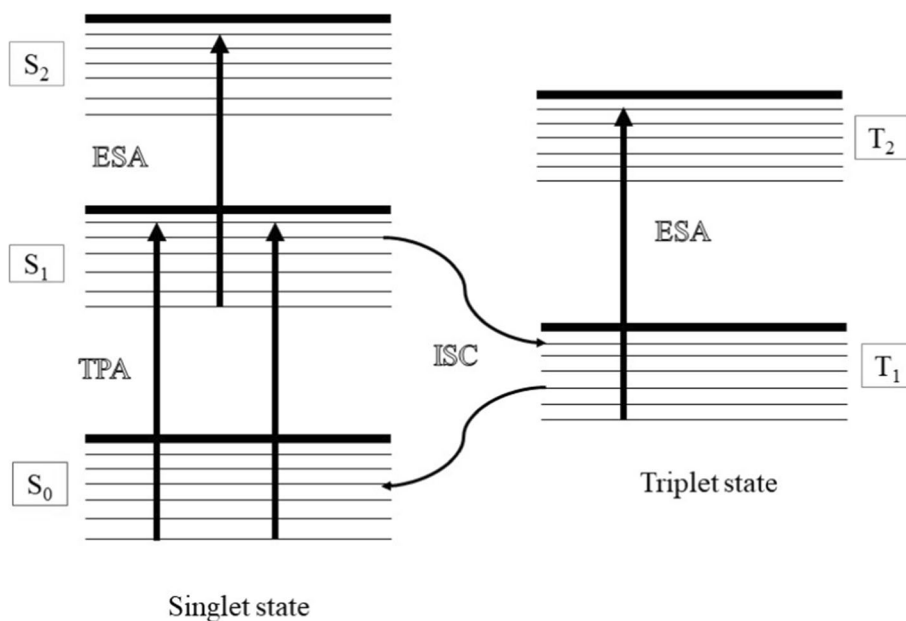
Fig. 8 Open-aperture Z-scan curves obtained for AG 3 in water and AG 3-PVA films

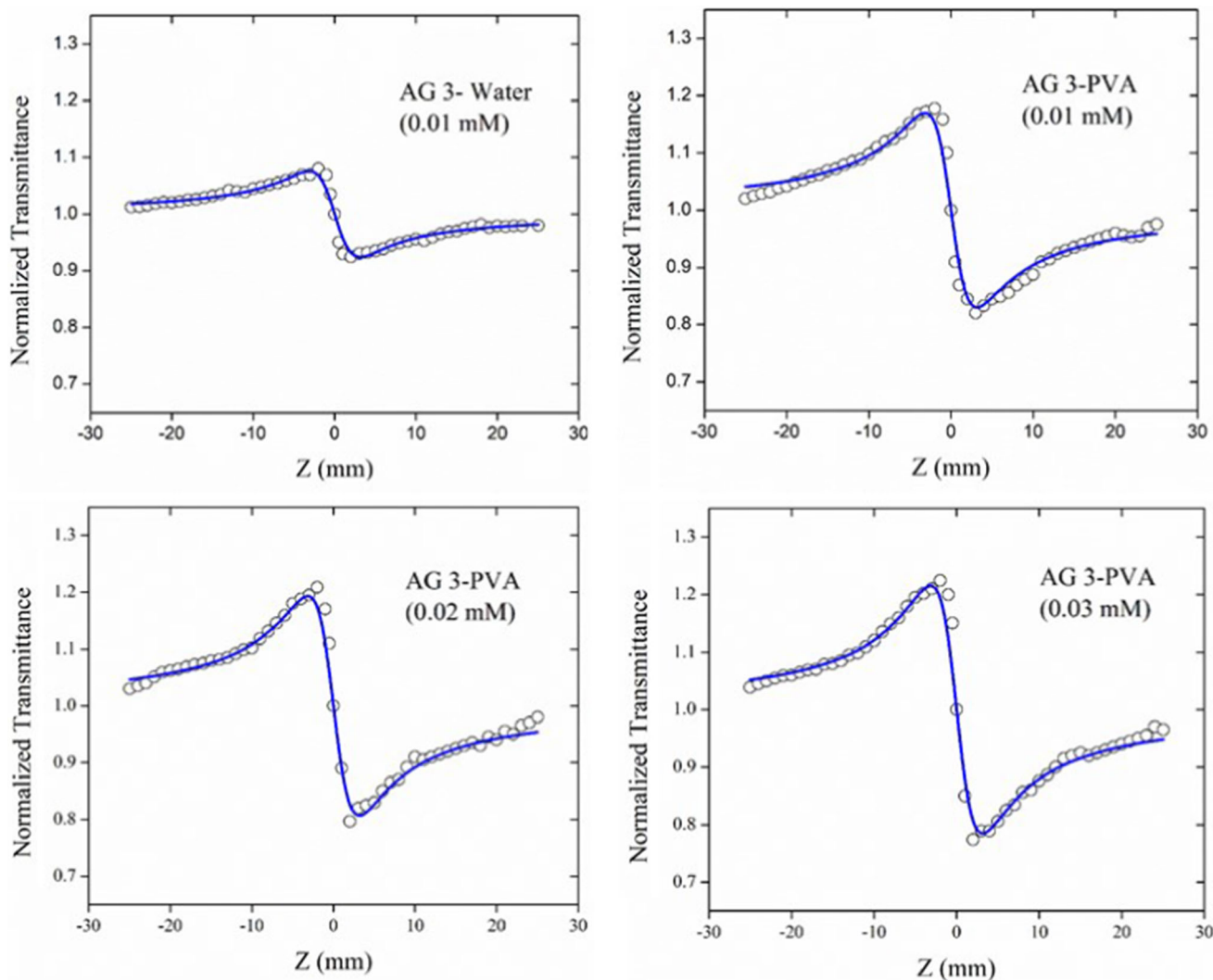**Fig. 9** Five-level model energy diagram for AG 3 dye molecule

Fig. 10 Pure nonlinear refraction Z-scan curves obtained for AG 3 dye in water and AG 3-PVA films

absorption. Harilal et al., George et al. [38, 39] stated the RSA behavior in organic dyes. Figure 9 shows the five-level model of energy diagram can be used to substantiate the NLA performance in organic dye molecules. Singlet ground, singlet first excited state and singlet next higher excited state are represented by S_0, S_1 and S_2, respectively, Likewise, T_1 and T_2 are triplet first and triplet higher excited states, respectively. TPA is defined as the simultaneous absorption of two photons of the same or different energies from the ground state to higher-energy excited state (S_0–S_1). When an electron is stimulated to the lower excited state, ESA occurs (S_1–S_2 and/or T_1–T_2). To do this, the population of excited states (S_1 and/or T_1) must be large enough to increase the probability of absorbing a photon from the state. Transitions to T_2 may be feasible if electrons from S_1 are shifted to T_1 via intersystem crossover (ISC), improving the ESA or RSA.

The nonlinear absorption coefficient β can be estimated from the fitting curve (Fig. 8) of the open-aperture Z-scan data using the relation,

$$T(z, s = 1) = \sum_{m=0}^{\infty} \frac{[-q_0(z)]^m}{[m+1]^{\frac{3}{2}}}, \text{for} |q_0(0)| < 1 \quad (1)$$
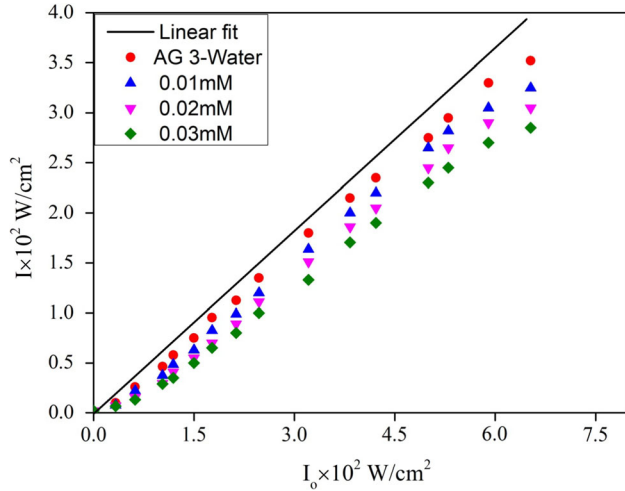
where

$$q_0(z) = \frac{\beta_{\text{eff}} I_0 L_{\text{eff}}}{1 + \frac{z^2}{z_0^2}} \quad (2)$$

where L_{eff} is the effective thickness of the sample, which is defined as, $L_{\text{eff}} = \frac{(1 - e^{-\alpha L})}{\alpha}$, I_0 is the intensity of the laser beam at the focus, α is the linear absorption coefficient and L is the thickness of the sample.

The closed-aperture Z-scan experiments have been performed with an aperture ($S = 0.4$) to study the nonlinear refraction (NLR) behavior of the aqueous solution of AG 3

Table 2 Measured third-order NLO parameters of AG 3 dye in water and AG 3-PVA films (Incident intensity $I_0 = 1.135 \times 10^3$ W/cm^2)

Sample	Dye concentration (mM)	ΔT_{P-V}	$n_2 \times 10^{-8}$ (cm^2/W)	$\beta \times 10^{-1}$ (cm/W)	$\chi^{(3)} | \times 10^{-5}$ (e.s.u)
AG 3–water	0.01	0.15	0.038	0.018	0.041
Solution	0.01	0.32	4.45	2.78	6.31
AG 3-PVA					
AG 3-PVA	0.02	0.37	4.58	3.71	8.41
AG 3-PVA	0.03	0.41	4.62	4.39	9.96

Fig. 11 Optical limiting behavior of AG 3 dye in water and AG 3-PVA films

dye and AG 3-PVA films. Figure 10 illustrates the pure nonlinear refraction Z-scan curves obtained for the aqueous solution of AG 3 dye and AG 3-PVA films with different dye concentrations. The pre-focal transmittance maximum (peak) followed by a post-focal transmittance minimum (valley) was obtained from the closed-aperture Z-scan data for the AG 3-PVA films and the aqueous solution of AG 3 dye. This peak–valley point indicates the signature of self-defocusing type nonlinearity which corresponds to negative nonlinear refractive index [40, 41]. In the present case, the excitation of CW laser light induces self-defocusing nonlinearity which may arise from the thermal origin.

The n_2 of the sample can be estimated from the obtained fitting curve (Fig. 10) of the closed-aperture Z-scan data using the relation,

$$T(z) = 1 - \Delta\varphi_0 \frac{4X}{(X^2 + 1)(X^2 + 9)} \tag{3}$$

where $X = Z/Z_0$. The nonlinear refractive index n_2 can be determined using the relation given by

$$n_2 = \frac{\Delta\varphi_0 \lambda}{2\pi I_0 L_{\text{eff}}} \left(\frac{cm^2}{W} \right) \tag{4}$$

where λ is the laser wavelength, $I_0 = 1.135$ kW/cm^2 is the input intensity and L_{eff} is the effective length of the sample. The real and imaginary parts of the third-order NLO susceptibility $\chi^{(3)}$ are given by,

$$\text{Re}\left[\chi^{(3)}\right](\text{esu}) = 10^{-4} \frac{\varepsilon_0 c^2 n_0^2}{\pi} n_2 \left(\frac{cm^2}{W} \right) \tag{5}$$

$$\text{Im}\left[\chi^{(3)}\right](\text{esu}) = 10^{-2} \frac{\varepsilon_0 c^2 n_0^2 \lambda}{4\pi^2} \beta \left(\frac{cm}{W} \right) \tag{6}$$

where ε_0 is the permittivity of free space and c is the velocity of light in vacuum. The third-order NLO susceptibility $\chi^{(3)}$ of the AG 3-PVA films was calculated using the real and imaginary parts of the $\chi^{(3)}$ values.

The measured NLO parameters such as the nonlinear refractive index n_2, nonlinear absorption coefficient β and real and imaginary parts of the third-order NLO susceptibility $\chi^{(3)}$ for AG 3-PVA films and the aqueous solution of AG 3 dye are given in Table 2. From Table 2, It is observed that there is an increased ΔT_{p-v} values for AG 3–PVA films than that of aqueous solution of AG 3 dye; this may be due to the fact that heat dissipation rate is faster in liquids than that of solid film. This may be due to the fact that heat dissipation rate is faster in liquids than that of solid film. It is clear from the results that the measured NLO parameters of n_2 and β are linearly dependent on dye concentrations and these parameters get increased as the dye concentration increases in the AG 3-PVA matrix. This may be due to the fact that with the increase in weight percentage of the dye molecules, the number of participating light-sensitive particles increases which in turn enhances the optical nonlinearity. As the AG 3-PVA film is illuminated by CW diode laser, a minimal portion of its energy is absorbed by the particles in the film; at higher concentrated films, more number of particles may thermally be agitated due to the local heating which results in temperature variation or the nonlinear index of refraction in the sample medium [42].

3.5. Optical power limiting

Optical limiting (OL), a process in which the beam transmittance through a material decreases as the input light intensity increases, is one of the most important uses of NLO materials. An ideal optical limiter has high linear transmission for low light input intensities; however, once the input intensity reaches the threshold, the transmitted light intensity becomes constant. Optical limiters protect our eyes, optical equipment and optical sensors from powerful laser beams. A good optical limiter must endure the qualities of high linear transmission, low limiting threshold level, fast response time, broadband limiting response and low light scattering. The optical limiting measurements for the present samples were taken using an open-aperture configuration method, in which the sample was kept at the focal plane of the lens and the input intensity of the laser beam was adjusted with a neutral density filter (NDF), while the corresponding transmitted intensity was determined with an optical power meter. Optical power limiting behavior of the aqueous solution of AG 3 dye and AG 3-PVA films with different dye concentrations of 0.01 mM, 0.02 mM and 0.03 mM and the aqueous solution of AG 3 dye has been studied, and the results are presented in Fig. 11. At low input light intensities, a linear curve has been obtained between the input and output light intensities for AG 3-PVA films and the aqueous solution of AG 3 dye, which obeys the conditions of Beer's law. It is obvious that when increasing the concentration of the dye in the polymer matrix, the corresponding limiting threshold value gets decreased. The samples that we have chosen for the present study have good optical qualities or transparencies at the excitation wavelength of 635 nm. Much higher concentrated samples may not be applicable for the present experiment as the laser used has a limited maximum power of 5 mW. In the case of higher concentration of AG 3 dye, the samples may become darker or optically opaque, as it includes more dye molecules, which may require higher excitation light intensity. We have aimed for measuring the nonlinear optical (NLO) properties and the optical limiting behavior of acid green 3-PVA films for suitable applications in NLO devices working in low-power regime. The straight line shown in Fig. 11 is for the reference, from where one could observe a smaller deviation from linear line for each sample. For little more or higher concentrated samples with the usage of higher laser powers, the optical limiting threshold and the saturation points may be more visible. Generally, organic dyes which exhibit reverse saturable absorption (RSA) characteristics will certainly suitable for optical limiting applications. Optical limiting can be attained by numerous nonlinear phenomena such reverse saturable absorption (RSA), two-photon absorption (TPA), excited state absorption (ESA) and photo-refraction [32]. The observed limiting behavior for AG 3-PVA films is mostly due to RSA, an energy absorbing optical limiter, as validated by open-aperture Z-scan measurements for the samples.

4. Conclusions

Acid green 3 dye-doped poly(vinyl alcohol) films have been prepared using the solution cast method, and their structure, morphology, linear, nonlinear optical (NLO) and power limiting characteristics were studied. FT-IR analysis indicates the occurrence of weak bonding interaction between dye molecules and PVA in the AG 3-PVA film. The microstructure studies reveal that the features of surface topography with uniform distribution of nanoclusters of varying sizes all over the surface of AG 3-PVA films and the morphology show an agglomeration of particles in the dye polymer matrix. AG 3-PVA films exhibit the thermally originated optical nonlinearity with $\chi^{(3)}$ value of the order of 10^{-5} esu and an optical limiting characteristic behavior. With these results, we suggest that the present AG 3-PVA films may be suitable for potential applications in optical limiting, photonics and optoelectronics devices.

References

[1] M A Kramer Rev. A 34 2026 (1986)
[2] E Holder J. Mater. Chem. 18 1064 (2008)
[3] G P Agarwal and R W Boyd Contemporary Nonlinear Optics Quantum Electronics-Principles and Application Series (New York) (1992)
[4] J L Bredas, C Adant, P Tackx and A Persoons Chem. Rev. 94 243 (1994)
[5] H S Nalwa Adv. Mater. 5 341 (1993)
[6] G Ravindra Kumar and F A Rajgara Appl. Phys. Lett. 67 3871 (1995)
[7] T Geethakrishnan and P K Palanisamy Optik 117 282 (2006)
[8] T Geethakrishnan and P K Palanisamy J. Phys. 66 473 (2006)
[9] B Sahraoui, J Luc, A Meghea, R Czaplicki, J L Fillaut and A Migalska-Zalas J. Opt. A: Pure Appl. Opt. 11 1 (2009)
[10] S K Yesodha, S Pillai and N Tsutsumi Prog. Polym. Sci. 29 45 (2004)
[11] S Zahedi and D Dorranian Opt. Rev. 20 36 (2013)
[12] Z H Esfahani, M Ghanipour and D Dorranian J. Theor. Appl. Phys. 8 117 (2014)
[13] M Obula Reddy and B Chandra Babu Indian J. Mater. Sci. 1 927364 (2015)
[14] P G L Frobel, S R Suresh, S Mayadevi, S Sreeja, C Mukherjee and C I Muneera Mater. Chem. Phys. 129 981 (2011)
[15] A Ishchenko Pure Appl. Chem. 80 1525 (2008)
[16] V Viswanath, S Sreeja, G Subodh and C I Muneera SN Appl. Sci. 1 1 (2019)
[17] K M Manikandan, A Yelilarasi, P Senthamaraikannan, S Saravanakumar, A Khan and M Abdullah Int. J. Polym. Anal. Charact. 326 1 (2019)

[18] T S Soliman, S A Vshivkov and J Non *Cryst Solids.* **519** 119452 (2019)

[19] F M Ali and R M Kersh *Matter.* **538** 160 (2018)

[20] I Qashou, E F M El Zaidia, A A A Darwish and T A Hanafy *Physica B Condens Matter.* **571** 93 (2019)

[21] S Adhikari *Synth. Met.* **159** 2519 (2009)

[22] M Sheik-Bahae, A A Said and E W Van Stryland *Opt. Lett.* **14** 955 (1989)

[23] S Zongo, K Sanusi, J Britton, P Mthunzi, T Nyokong, M Maaza and B Sahraoui *Opt. Mater.* **46** 270 (2015)

[24] I Elashmawi, E Abdelrazek and I Appl *Polym. Sci.* **115** 2691 (2010)

[25] A T Slark and P M Hadgett *Polymer* **40** 1325 (1999)

[26] K E Strawhecker and E Manias *Macromolecules* **34** 8475 (2001)

[27] T Hanemann and D V Szabo *Materials* **3** 3468 (2010)

[28] D S Seo, H Kim and J K Lee (2007) Key Eng. Mater. 1553

[29] H M Ragab *Results Phys.* **7** 2057 (2017)

[30] S Zongo, M S Dhlamini, P H Neethling and A Yao *Mater.* **50** 138 (2015)

[31] S Ningaraju and H B Ravikumar *J. Polym. Res.* **24** 1 (2017)

[32] T Geethakrishnan and P K Palanisamy *Opt. Commun.* **270** 424 (2007)

[33] T Geethakrishnan and P K Palanisamy *Curr. Sci.* **89** 1894 (2005)

[34] T Geethakrishnan and P K Palanisamy *Appl. Phys. B* **82** 169 (2006)

[35] R K Choubey, S Medhekar and R Kumar *J. Mater. Sci. Mater. Electron.* **25** 1410 (2014)

[36] T Geethakrishnan and P K Palanisamy *Mod. Phys. Lett. B* **20** 245 (2006)

[37] T Geethakrishnan and P K Palanisamy *J. Mod. Opt.* **53** 1131 (2005)

[38] M George and C I Muneera *Laser. Technol.* **40** 373 (2008)

[39] S S Harilal and C V Bindhu *J. Appl. Phys.* **86** 1388 (1999)

[40] K J Ghaleh, S Salmani and M H M Ara *Opt. Commun.* **271** 551 (2007)

[41] R K Rekha and A Ramalingam *J. Sci. Technol* **2** 27 (2009)

[42] R Madhana Sundari and P K Palanisamy *Appl. Surf. Sci.* **252** 2281 (2006)